ACTA NEUROBIOLOGIAE EXPERIMENTALIS

Research paper Acta Neurobiol Exp 2010, 70: 246–260

Sepsis induces apoptotic cell death in different regions of the brain in a rat model of sepsis

Ilker M. Kafa, Murat Uysal, Sinan Bakirci, and M. Ayberk Kurt*

Uludag University, Faculty of Medicine, Anatomy Department, Bursa, Turkey; *Email: ayberk@uludag.edu.tr

Sepsis occurs in 14-37% of patients admitted to intensive care units and sepsis associated encephalopathy (SAE) is its severe complication. In an attempt to provide insight into the question how sepsis and SAE contributes cerebral dysfunction, apoptotic cell death was investigated in hippocampal formation, centers of adult neurogenesis and main autonomic centers which are known to regulate heart rate, respiration and other visceral activities, in cecal ligation and puncture (CLP) rat model of sepsis. Vital parameters and electrophysiological changes were monitored for the confirmation of sepsis and SAE, respectively. Apoptotic cell death was evaluated by TUNEL staining, Caspase-3 immunohistochemistry and transmission electron microscope (TEM). Significantly higher number of TUNEL positive apoptotic cells in the median preoptic nucleus, subventricular zone, dentate gyrus and CA1 and CA3 regions of the hippocampal formation were observed in CLP group and Caspase-3 immunohistochemistry and TEM findings were in line with these results, suggesting that the apoptotic cell death would bare a major role in the pathogenesis of the SAE.

Key words: apoptosis, brain, Caspase-3, sepsis associated encephalopathy, TUNEL

INTRODUCTION

Sepsis is one of the most significant challenges in critical care. With standard supportive care alone, mortality remains unacceptably high, at 28-50% (Natanson et al. 1998). Increased research into the molecular mechanisms of sepsis has brought greater understanding of its pathophysiology. Evidence suggests that sepsis is a disease of the microvasculature and microvascular dysfunction is characterized by: decreased perfusion and oxygen availability (Lam et al. 1994, McGilvray and Rotstein 1998), endothelial dysfunction and increased capillary permeability (Aird 2003), reduced vasomotor tone (McCuskey 1996) and increased leukocyte-endothelium interactions (Sugama et al. 1992, Rahman et al. 1999).

Sepsis associated encephalopathy (SAE) is a severe complication of sepsis with an incidence ranging from 9% to 71%. SAE manifests itself with varying degree of brain dysfunction ranging from confusion to coma and it's associated with increased morbidity and mortality (Papadopoulos et al. 2000, Wilson and Young 2003, Consales and De Gaudio 2005). Although, diagnosis of SAE relies mainly on neurologic examination, an electroencephalogram and somatosensory evoked potentials (SEP) can also be useful for the detection of brain dysfunction (Siami et al. 2008). The pathophysiology of SAE is still incompletely known and the mechanism proposed in the pathogenesis of SAE involves: microorganisms directly invading the CNS or affecting it with their toxins (Hotchkiss et al. 1989, Orlikowski et al. 2003), metabolic alterations that could adversely affect CNS function (Soejima et al. 1990, Basler et al. 2002), breakdown of blood brain barrier (Davies 2002, Ari et al. 2006, Kafa et al. 2007), altered neurotransmitter synthesis and receptorial distribution (Freund et al. 1985, Winder et al. 1988, Kadoi et al. 1996, Davies et al. 2001), impairment of brain circulation and auto-regulatory power (Bowton et al. 1989, Wijdicks and Stevens 1992, Terborg et al. 2001, Booke et al. 2003).

The importance of apoptosis in the immunopathogenesis of sepsis is well established and increased apoptotic death of various parenchymal cells in vari-

Correspondence should be addressed to M. A. Kurt
E-mail: ayberk@uludag.edu.tr

Received 9 March 2010, accepted 14 August 2010

ous organs: e.g., endothelial cells, hepatocytes, gastrointestinal and lung epithelial cells and cardiac myocytes has been indicated in clinical and experimental sepsis (Kim et al. 2000, Mutunga et al. 2001, Coopersmith et al. 2002, Perl et al. 2005, 2007, Gambim et al. 2007, Wesche-Soldato et al. 2007, Ayala et al. 2008). However, studies that investigate its role in the pathopyhsiology of SAE is limited although it's reasonable to suggest that the parenchymal cells of the central nervous system are affected in a similar way by TNF-α and/or other cytokines released in sepsis (Mouihate and Pittman 1998, Messaris et al. 2004, 2010, Sharshar et al. 2004, Semmler et al. 2005, Memos et al. 2009). With this in mind, apoptotic cell death was investigated in hippocampal formation, centers of adult neurogenesis and main autonomic centers which are known to regulate heart rate, respiration and other visceral activities, in a rat model of sepsis by using terminal deoxyribonucleotidyl transferase-mediated dUTP-biotin nick end-labeling (TUNEL), Caspase-3 immunohistochemistry and electron microscopy, in an attempt to provide insight into the question whether apoptosis contributes to cerebral dysfunction and SAE in sepsis.

METHODS

Animals

Adult Wistar rats weighing 270±30 g were used in this study. Rats were obtained from the Experimental Animals Breeding and Research Centre of Uludag University Medical Faculty. All experimental protocols were approved according the guidelines of the Animal Care, Use and Ethics Committee of Uludag University and carried out in accordance with the European Communities Council Directive. The rats were housed one per cage at 20-24°C under a 12:12-h light:dark regime and received standard laboratory chow and tap water ad libitum. All rats were anesthetized by intraperitoneal injection of 50 mg/kg thiopental sodium and held under anesthesia during the entire surgical procedures in order to minimize any pain or discomfort.

Vital parameters, neurological investigations and light microscope studies were carried out on a total of 33 rats which were assigned into one of the following three groups: Cecal Ligation and Puncture (CLP) group, sham-operated and un-operated control group (n=8 for each group). Nine rats which did not survive the CLP procedures were excluded from these studies. Another set of eleven rats, which consisted four sham-operated and four CLP rats in the end, were used for electron microscopic investigations.

Induction of sepsis

Induction of sepsis was performed using a CLP model as previously described (Wichterman et al. 1980). Briefly, under sterile surgical conditions, a 2 cm abdominal incision was made along the ventral surface of the abdomen to expose the cecum, which was then ligated below the ileocecal junction without causing bowel obstruction. Cecum was then punctured twice with a 22-gauge needle and fecal contents were allowed to leak into the peritoneum by gently squeezing the cecum. The bowel is then returned to the abdomen and the abdominal cavity was closed. Sham-operated animals were submitted to laparotomy and the cecum was manipulated but neither ligated nor punctured, while no surgical intervention is performed in un-operated control group. All animals underwent surgical manipulation, received a subcutaneous injection of saline solution (3 ml/100 g body weight) and the incision site is cleaned with an antiseptic solution (10% polyvinylpyrrolidone iodine) at the end of surgery. A topical antibiotic (2% Nitrofurazone) also applied to the surgical site every 6 hours.

Evaluation of vital parameters

Blood pressure, heart rate and rectal temperatures were recorded before (0h) and at 2, 6, 12 and 24 hours after the surgery using invasive methods to confirm the development of sepsis findings in CLP group. The blood pressure was recorded as mean arterial blood pressure (MAP-mmHg) and measured by using a computerized tail-cuff system connected to a volumetric pressure transducer (MIBP200A, Biopac Systems, CA, USA) attached to a polygraph (Mp150, Biopac Systems, CA, USA) and a PC running a data analysis software (AcqKnowledge, 3.7). Heart rate was then estimated from the blood pressure waves on the polygraph tracings and recorded as beats/min. Rectal temperature was recorded using a rectal probe (TSD202F, Biopac Systems Inc., CA, USA) connected to an amplifier (ST100C temperature unit, Biopac Systems Inc., CA, USA), a transducer (TSD202F) and the same data acquisition system (Mp150).

Neurological assessment and evaluation of brains electrical activity

CLP rats were also neurologically assessed and scored by checking various reflexes. Electrocorticographic (ECoG) waves and somatosensory evoked potentials (SEPs) were also recorded before (0h) and at 2, 6, 12 and 24 hours after the surgery for the analysis of the brains electrical activity and confirmation of the development of encephalopathy findings. Neurological reflexes evaluated were; the Pinna reflex and the corneal reflex for the evaluation of simple nonpostural somatomotor function, tail flexion reflex for the evaluation of simple postural somatomotor function and finally righting reflex and escape response for evaluation of complex postural somatomotor function (Habernam et al. 1999). The Pinna reflex was assessed by lightly touching the auditory meatus of the ear to elicit a vigorous head shake, the corneal reflex was evaluated by lightly touching the cornea with a cotton swab to elicit a head shake, the tail flexion and the escape response reflex was assessed by briefly pinching the tail to elicit a withdrawal response and elicit locomotive activity away from the noxious stimulus, respectively and finally the righting reflex was tested by placing the animal on its back and measuring the time taken to return to a spontaneous upright position. A "0" score was given for no reflex; "1" for weak reflex (loss of reflex for 10 sec), "2" for normal reflex; with a maximal obtainable score of 10 points for each rat.

For electrophysiological recordings, under sterile surgical conditions and the sodium thiopental anesthesia (50 mg/kg, ip), three 0.6 mm stainless steel screws (Plastics One Inc, Roanoke, VA, USA) were implanted as epidural electrodes in the undersized holes drilled in the skull as previously described in detail (Habernam et al. 1999) ten days prior to surgical intervention. Briefly, one of the electrodes was placed on primary somatosensory (S1) cortex (2.5 mm posterior to bregma and 2.5 mm laterally from the sagittal suture on the right side). Remainder two of the electrodes were installed bilaterally above the frontal sinus (10 mm anterior to bregma and 1 mm lateral to each side of midsagital plane); the one on the left side serving as the ground. Electrodes were wired to a receptacle (MS333/2A, Plastics One, USA), fixed to the skull using dental cement and the skin was sutured. ECoG recordings were obtained using S1 electrode referred to ipsilateral frontal electrode. The signals amplified by an amplifier (EEG100C, Biopac Systems Inc., CA, USA) and recorded (band pass 0.5–130 Hz, 120 second) by a data acquisition system (Mp150 Data Acquisition system, Biopac Systems Inc., CA, USA) and processed with AcqKnowledge 3.7 software (Biopac Systems Inc., CA, USA). The power spectra obtained by use of Fast Fourier transform (FFT) were divided into 0.5-3 Hz (delta), 4-8 Hz (theta), 8-13 Hz (alpha), and 13-30 Hz (beta) frequency bands and Median Power Frequency (MF = the frequency below which 50% of the power) were also calculated using data acquisition software.

SEPs were evoked by electric stimulation using stimulation two stimulation electrodes (27G needles) fitted firmly in the middle third of tail on the left side, 2 mm away from each other. The stimuli were 2 ms square wave pulses which were triggered by the data acquisition software (AcqKnowledge 3.7, Biopac Systems Inc., CA, USA) and generated by a stimulator (Mp150 Data Acquisition system, Biopac Systems Inc., CA, USA). SEPs were recorded from the SI electrode using the same data acquisition system and a biopotential amplifier (EEG100C, Biopac Systems Inc., CA, USA) as ipsilateral frontal sinus electrode served as reference electrode and the contralateral frontal sinus electrode served as signal ground. Total of 100 signals were band-pass filtered between 15 and 300 Hz, amplified 2000 times, averaged in real time at 2 kHz, stored and analyzed by the same data acquisition software. Measurements were made on two positive potentials (P1 and P2) and one negative potential (N1). Baseline to peak amplitudes and peak latencies were calculated.

Tissue removal and processing

After the last monitoring procedures completed at 24th hour, the rats were given a lethal dose of anaesthetic and perfused through the left cardiac ventricle with 0.9% NaCl followed by a fixative solution containing 4% paraformaldehyde and 0.1% glutaraldehyde in 0.1 M phosphate buffer saline (PBS) pH 7.4. The brains were then removed and immersed overnight in a fixative containing 2% paraformaldehyde and 2.5% glutaraldehyde in 0.1 M PBS (pH 7). The brains were then placed in a matrix and three 2mm thick coronal slices were taken from each brain, with reference to Bregma +1 mm to –1 mm, –2 mm to –4mm and

–11mm to –13 mm, respectively (Paxinos and Watson 1997). Each slice was then processed into paraffin wax, cut coronally into 5 µm thick sections. Two consecutive sections in every ten section are collected and mounted on two different slides. Apoptotic cell death is then investigated for each rat, using TUNEL and caspase-3 immunohistochemistry in ten different regions of the brain in a total of six and two sections, respectively. Brain regions investigated were: hippocampal formation (CA1, CA3 and dentate gyrus), centers of adult neurogenesis (subventricular zone and dentate gyrus) and main autonomic centers (median preoptic nucleus, insular cortex, zona incerta, perifornical nucleus, nucleus of the solitary tract and intermediate reticular nucleus) which are known to regulate heart rate, respiration and other visceral activities. Coronal slices and the brain regions investigated for apoptotic cell death in each slice are shown in Figure 1.

TUNEL and Caspase-3 staining

For TUNEL staining, tissue sections were deparaffinized, rehydrated through a series of graded alcohols, washed in distilled water followed by PBS. Subsequently, the sections were permeabilized using proteinase K (20 µg/ml, 20 min at room temp.), washed in PBS, incubated in 2% H_2O_2 in 0.1 M PBS for 30 min at room temperature in order to quench endogenous peroxidase activity and treated with Triton-X. The terminal deoxynucleotide transferase-mediated dUTP nick end labeling (TUNEL) reaction performed using the In Situ Cell Death Detection Kit (Roche, Mannheim, Germany). Briefly, the slides were incubated with TUNEL reaction mixture for 60 min (humid chamber, 37ºC), and then were washed twice in PBS. After multiple washing steps, the sections were treated with Converter-POD solution for 30 min (humid chamber, 37ºC), rinsed with PBS and they visualized by adding 3,3'-diaminobenzine (DAB) for 10 min at room temperature, and then washed in phosphate buffer saline (PBS), counterstained using hematoxylin staining and finally mounted for light microscopic observation. For positive controls, sections were incubated with DNase I for 10 minutes at 15-25ºC to induce DNA strand breaks, prior to labeling procedure. For negative controls, sections were incubated with label solution only (without terminal transferase) instead of TUNEL reaction mixture. A Sony Cybershot DSC-F717 digital camera attached to a Nikon 4S-2 Alphaphot light microscope and PC running Scion-Image software (public domain, version 4.02) were used to capture images and determine the number of TUNEL positive cells. Only TUNEL positive cells with a condensed pyknotic cells, which were stained intensely with DAB were marked and counted in an area of 1mm^2 using 400× microscopic magnifications. The averages of six histological sections for each rat were reported as mean ± S.E.M. All morphometric measurements were carried out in a blinded manner and expressed in comparison to controls.

For immunohistochemical detection of active caspase-3, sections were subjected to the antigen retrieval by microwave treatment (10 min, 700W, in 10 mM

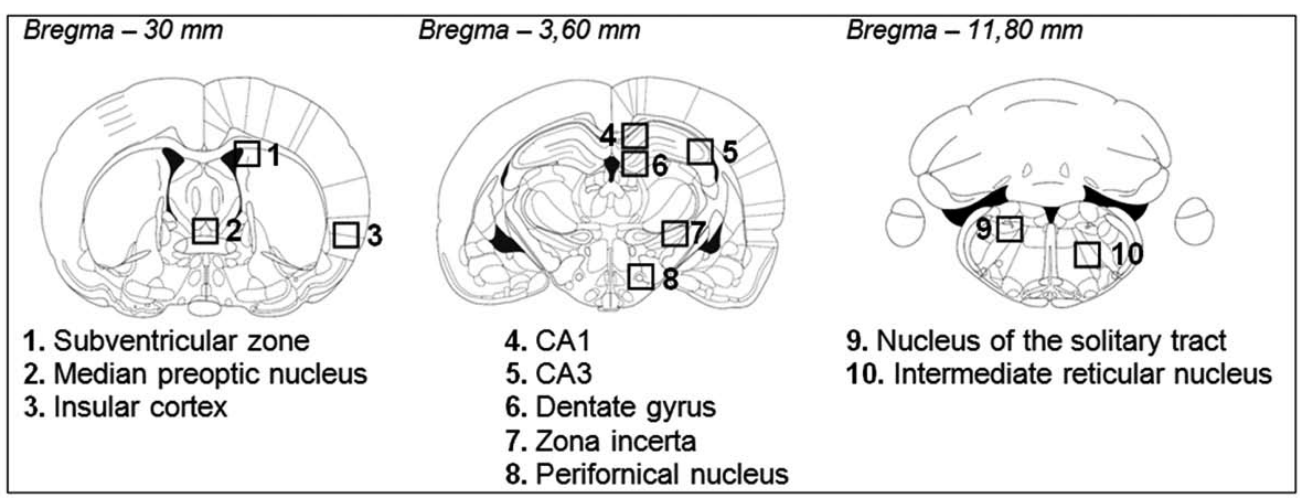

Fig. 1. Line diagrams (reproduced from Paxinos and Watson 1997) to show the orientation of coronal tissue slices and the brain regions investigated for apoptotic cell death taken from cecal ligation and puncture and control groups.

Table I

Vital parameters, neurological scorings, electrocortigographic (ECoG) and somatosensory evoked potential (SEP) recordings.

	HOURS				
	0	2	6	12	24
VITAL PARAMETERS					
Mean Arterial Pressure (mmHg)	108,88 ± 8,7	114,11 ± 15,8	106,50 ± 0,75	95,72 ± 9,9	59,73 ± 1,94*
Heart Rate (beats per min)	350,02 ± 8,1	386,02 ± 32,4	430,55 ± 0,9*	429,51 ± 11,8*	456,26 ± 15,4*
Rectal Temperature (ºC)	36,95 ± 0,3	35,90 ± 0,6	37,05 ± 0,75	37,25 ± 0,75	37,00 ± 0,3
NEUROLOGICAL SCORINGS					
Neurological Score (0-10)	10 ± 0	0*	*2* ± 0,1*	*6* ± 0,5*	*7* ± 0,2*
ECoG RECORDINGS					
Median Power Frequency (Hz)	13,38 ± 1.3	14,54 ± 1.1	13,82 ± 0,6	12,27 ± 0,3	10,60 ± 0,8
Beta Frequecy (Spectral Power %)	36,67 ± 2,3	38,02 ± 0,7	35,47 ± 2,7	34,08 ± 0,4	30,33 ± 2,1
Delta Frequecy (Spectral Power %)	16,70 ± 2.2	16,06 ± 1,8	17,18 ± 1,8	21,81 ± 2.4	27,64 ± 3,5*
SEP RECORDINGS					
P1 Amplitude (μV)	16,14 ± 1,7	14,01 ± 3,2	11,92 ± 0.4*	14,67 ± 0,6	11,73 ± 0,6*
S-P1 Latency (% difference)	100.00 ± 0	99,46 ± 2,3	107,18 ± 6,1*	111,10 ± 1,5*	109,89 ± 2,3*
P1-N1 Latency (% difference)	100.00 ± 0	100,65 ± 0,6	98,63 ± 1,8	100,00 ± 1,9	100,66 ± 2.5
N1-P2 Latency (% difference)	100.00 ± 0	110,00 ± 5,9*	117,76 ± 10,9*	114,32 ± 10,3*	114,53 ± 11,3*

Mean values ± the standard error of the means (SEM) of vital parameters, neurological scorings, electrocortigographic (ECoG) and somatosensory evoked potential (SEP) results recorded from cecal ligation and puncture group at 0, 2, 6, 12, and 24 hours after the surgery. *; $p < 0.05$ and represents significance compared to baseline values.

Citrate Buffer), following the dehydration. To remove endogenous peroxidase activity, sections were treated with 3% hydrogen peroxide for 30 min. After non-specific blocking with the goat serum for 30 min, the sections were incubated with primary antibodies against active caspase-3 (diluted 1:100, Chemicon, AB3623-rabbit, USA) for overnight at 4ºC, followed by the treatment with biotinylated anti-rabbit secondary antibody for 30 min at room temperature. Following the Avidin-Biotin complex treatment, DAB was used for the color development. Negative control slides, omitting the primary antibody was also included. The tissue sections were examined, using a light microscope interfaced with a Sony Camera and scoring was

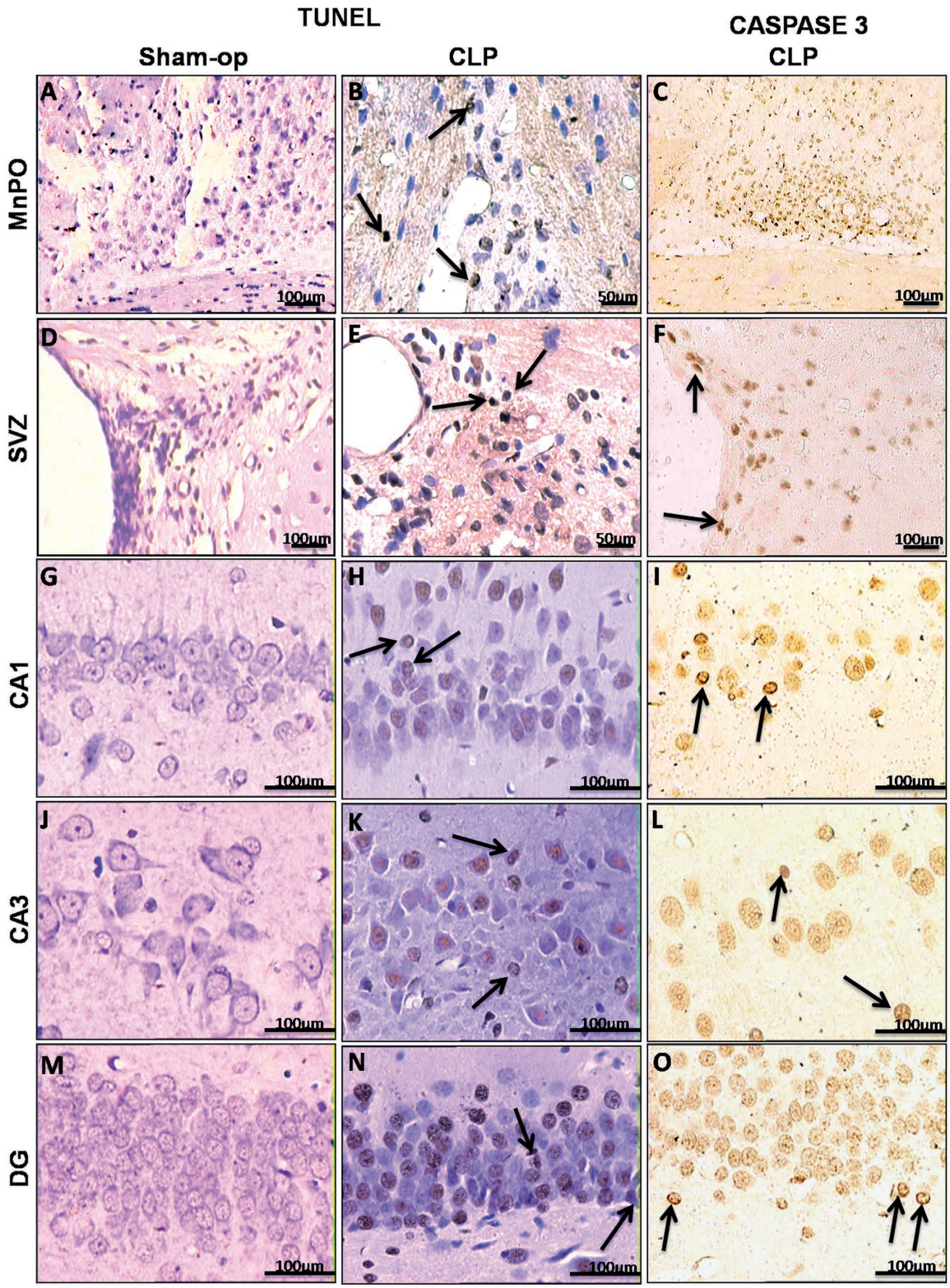

Fig. 2. Photomicrographs of examples of TUNEL and active Caspase-3 immunoreactive stained sections in the median preoptic nucleus (MnPO) **(A,B,C)**, subventricular zone (SVZ) **(D,E,F)**, CA1 **(G,H,I)**, CA3 **(J,K,L)** and dentate gyrus (DG) **(M,N,O)** of hippocampus in the sham-operated (sham-op) and cecal ligation and puncture rats (CLP). Arrows denote cells with characteristic morphology of apoptotic cells with shrunken cytoplasm and pyknotic nuclei.

Table II

TUNEL positive cell numbers ± the standard error of the means (SEM) in the median preoptic nucleus (MnPO), subventricular zone (SVZ), dentate gyrus (DG) and cornu ammonis (CA1+CA3) of individual un-operated, sham-operated and CLP operated rats.

	MnPO			SVZ		
Subject	Un-op	Sham-op	CLP	Un-op	Sham-op	CLP
1	0.14 ± (0.07)	0.43 ±(0.15)	16.14 ± (2.71)	0.64 ± (0.09)	0.86 ± (0.47)	20.00 ± (2.88)
2	0.23 ± (0.11)	0.34 ± (0.9)	19.00 ± (2.94)	0.20 ± (0.04)	0.48 ± (0.05)	8.69 ± (1.32)
3	0.18 ± (0.09)	0.10 ± (0.05)	5.44 ± (1.08)	0.12 ± (0.02)	0.64 ± (0.14)	18.61 ± (1.38)
4	0.44 ± (0.08)	0.30 ± (0.08)	8.29 ± (2.42)	0.07 ± (0.02)	0.72 ± (0.06)	7.71 ± (1.28)
5	0.26 ± (0.09)	0.31 ± (0.07)	0.03 ± (0.01)	0.27 ± (0.03)	0.30 ± (0.09)	7.50 ± (1.89)
6	0.52 ± (0.19)	0.38 ± (0.13)	0.23 ± (0.09)	0.17 ± (0.04)	0.66 ± (0.08)	2.06 ± (0.26)
7	0.20 ± (0.07)	0.65 ± (0.11)	0.20 ± (0.08)	0.41 ± (0.12)	0.61 ± (0.02)	0.09 ± (0.02)
8	0.11 ± (0.07)	0.17 ± (0.08)	0.12 ± (0.02)	0.14 ± (0.03)	0.22 ± (0.05)	0.08 ± (0.02)
	DG			CA1+CA3		
Subject	Un-op	Sham-op	CLP	Un-op	Sham-op	CLP
1	0.36 ± (0.28)	0.76 ± (0.23)	7.64 ± (0.48)	1.14 ± (0.18)	1.56 ± (0.15)	29.29 ± (0.52)
2	0.17 ± (0.03)	0.05 ± (0.02)	6.69 ± (0.56)	0.67 ± (0.11)	0.91 ± (0.09)	17.75 ± (1.49)
3	0.12 ± (0.05)	0.19 ± (0.06)	9.89 ± (1.95)	0.30 ± (0.04)	0.46 ± (0.08)	8.58 ± (1.16)
4	0.05 ± (0.01)	1.07 ± (0.04)	8.14 ± (1.57)	0.23 ± (0.01)	0.87 ± (0.15)	11.42 ± (1.90)
5	0.13 ± (0.03)	0.79 ± (0.08)	8.43 ± (2.65)	0.49 ± (0.04)	1.12 ± (0.09)	4.86 ± (1.21)
6	0.08 ± (0.02)	0.16 ± (0.08)	7.19 ± (1.63)	0.73 ± (0.04)	1.24 ± (0.13)	0.26 ± (0.01)
7	0.21 ± (0.05)	0.21 ± (0.09)	6.90 ± (1.61)	1.02 ± (0.04)	1.39 ± (0.14)	0.76 ± (0.14)
8	0.10 ± (0.02)	0.08 ± (0.02)	6.79 ± (1.08)	0.35 ± (0.03)	0.57 ± (0.09)	0.27 ± (0.03)

done by taking into account both the intensity of staining and the distribution (extent) of positively staining cells as previously described (Xu et al. 2004). Staining intensity was scored as 0 (negative), 1 (weak), 2 (moderate), and 3 (strong). Staining extent was scored as 0 (0%), 1 (1–25%), 2 (26–50%), 3 (51–75%), and 4 (76–100%) according to the percentage of cells staining positive for active caspase 3. The sum of the inten-

sity and extent of scores was calculated to estimate the final average staining scores (0–7). All slides were specially coded so that two independent investigator would be unaffected by the knowledge of their source.

Electron microscopy

For electron microscopy, four CLP rats with that developed the signs of sepsis and SAE together with four sham-operated rats were given a lethal dose of anaesthetic and perfused transcardially with 4% paraformaldehyde and 0.1% glutaraldehyde in 0.1 M phosphate buffer at pH 7.3. Their brains were then removed and immersed in similar fixative overnight. Two 2 mm thick coronal slices were taken from each brain, with reference to Bregma +1 mm to –1 mm and –2 mm to –4mm, respectively (Paxinos and Watson 1997). Each slice was then trimmed to produce a rectangular block of tissue (approximately 1mm wide), that contained MnPO and SVZ in the first and extending across the entire hippocampus and containing the DG, CA3 and CA1 in the second slice. Each tissue block was then post-fixed with 1% OsO_4 in 0.1 M phosphate buffer for 1 hour, dehydrated through a graded series of ethanols and embedded in Spurr's resin (Agar Scientific, Stansted, UK). Ultra-thin sections with gold interference colour (app. 80 nm) were then cut from the resin-embedded tissue blocks, picked up on copper grids and stained with uranyl acetate and lead citrate prior to investigation for the occurrence of apoptotic cells in a Jeol 100 electron microscope.

Statistical analysis

One-way repeated-measure ANOVA and Friedman repeated-measures ANOVA on ranks were used to evaluate the effect of surgical operation over time on the vital, ECoG, SEP parameters and neurological scorings. Kruskal Wallis test was used to compare the effect of surgical operation on TUNEL positive cell numbers and semi-quantitative Caspase-3 scores among groups. Post-hoc comparisons were made using the Mann-Whitney *U*-test. In each test, the data are expressed as the mean ± S.E.M. and $p<0.05$ is accepted as statistically significant. The effect of individual animal and surgical operation on TUNEL positive cells were further investigated by two-way analysis of variance.

RESULTS

Clinic and neurophysiologic findings

Approximately 50% of rats did not survive the CLP procedure during the 24 hour monitoring procedure. Approximately 90% of the surviving rats developed the clinical findings (piloerection, lethargy, flickering, ocular and nasal discharge) and vital signs (significantly decreased arterial pressure and increased heart beat) of sepsis at the end of the observation period. Among those, approximately 50% of the septic rats developed the signs and symptoms of encephalopathy evidenced by deteriorated neurological reflexes, decreased median and beta frequencies together with increased delta frequencies in electrocorticographical (ECoG) recordings, and decreased P1 activity accompanied with elongated latencies in SEP recordings 24 hours after surgery and only these rats are included in the CLP groups.

Mean values ± the standard error of the means (SEM) of mean arterial pressure, heart rate and rectal temperatures recorded at 0, 2, 6, 12, and 24 hours after the surgery from rats in the CLP group are presented in Table I. Mean Arterial Pressure (MAP) in CLP rats reflected a continuous decline starting from 2 hour after surgery and this reduction became significant at 12^{th} hour and grew to be even more manifest at 24^{th} hour compared to initial values recorded. A significant increase in heart rate at 6th hour, becoming even more prominent in the 12^{th} and 24^{th} hours was also recorded in CLP rats. Although an initial decline in rectal temperature was observed in CLP rats, the difference was not significant compared to initial values recorded in the remainder of the monitoring period. Finally, scorings of the neurological reflexes revealed a significant reflex loss, which persisted at 24^{th} hour after the surgery in CLP rats (Table I).

The results of the ECoG and SEP recordings obtained from rats included in the CLP group are also presented in Table I. Decline in the median power frequency was observed in CLP group at 24^{th} hour compared to initial values although the difference was not significant. When the power spectra were divided into 0.5-3 Hz (delta), 4-8 Hz (theta), 8-13 Hz (alpha), and 13-30 Hz (beta) frequency bands, a non-significant decrease in beta and a significant increase in delta ($p<0.05$) activities were observed at 24^{th} hr compared to initial values recorded in rats included in the CLP

group. Finally, SEP recordings revealed a significant decrease in P1 amplitude at 12th and 24th hour in CLP rats, together with significantly elongated S-P1 and N1-P2 latencies, starting from the 12th and 6th hours of the monitoring procedure, respectively ($p<0.05$, for all comparisons).

Morphological findings

TUNEL immunohistochemistry revealed a distinctive pattern of nuclear staining (Fig. 2) and the number of TUNEL positive cells were significantly higher in CLP group compared to sham-operated and non-operated controls in five regions among the ten brain regions investigated (Fig. 2,3). These regions were median preoptic nucleus (MnPO), subventricular zone of the lateral venticule (SVZ) and CA1, CA3 regions and dentate gyrus (DG) of hippocampus. Mean TUNEL positive cell numbers ± the standard error of the means (SEM) from individual rats in the unoperated, sham-operated and CLP group are presented in Table II. Two-way analysis of variance revealed that there was a significant effect of animal on TUNEL positive cell numbers for all five regions in CLP Group ($p<0.01$, for all regions). However, no significant effect of individual animal on TUNEL positive cell numbers was found in both un-operated and sham-operated control groups.

Evaluation of the density of apoptotic cells by Caspase-3 immunohistochemistry gave concordant results and Caspase-3 immunoreactive cells in these regions were significantly higher in CLP group compared to sham-operated and non-operated controls (Fig. 2,4). Caspase-3 immunoreactive cells usually had a normal appearance in keeping with the fact that Caspase-3 activation is an early phenomenon in apoptosis, proceeding DNA and terminal nuclear changes. However, part of them had the characteristic morphology of apoptotic cells with shrunken cytoplasm and pyknotic nuclei (Fig. 2, arrows).

Electron microscopic investigation of these five regions confirmed the presence of shrunken and pyknotic cells showing different aspects and phases of chromatin condensation and fragmentation within their nuclei as distinctive features of apoptosis (Fig. 5). Although the cytoplasmic membranes of these cells were usually intact, cytoplasmic blebbings, and some dying cells with disrupted cell membrane and apoptotic bodies were also observed (Fig.5). Electron microscopic investigation also showed the presence of distinctive perimicrovascular edema in CLP group in the regions investigated (Fig. 5I).

DISCUSSION

In the present study, we have investigated the effects sepsis and SAE onto the apoptotic cell death in the brains of CLP rats and demonstrated the presence of significantly more apoptotic cell death, in five regions (MnPO, SVZ, CA1, CA3 and DG) compared to sham-operated and un-operated controls. Our results also showed that CLP induces signs and symptoms of sepsis only in approximately 90% of these rats, which only 50% of them then demonstrated signs of encephalopathy.

Necessity of a uniform and valid definition of sepsis applicable to both small and large animals has previously been highlighted and its importance in preclinical sepsis studies has been underscored previously (Parker and Watkins 2001, Garrido et al. 2004). Compared to mechanisms such as endotoxicosis and intravenous bacterial infusion, peritonitis models have been proposed as the 'gold standard' in case of appropriate usage of virulent bacterial species (Fink and Heard 1990, Parker and Watkins 2001, Garrido et al. 2004). Although, peritonitis models developed in pigs (Doods 1982) and primates (Kinasewitz et al. 2000)

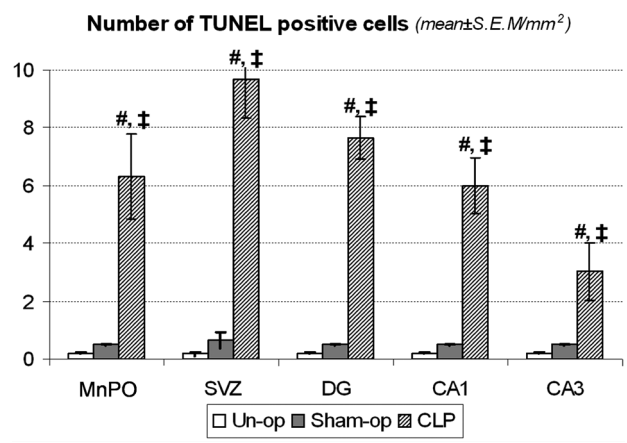

Fig. 3. A bar diagram showing the mean density (±SEM) of TUNEL positive cells in the median preoptic nucleus (MnPO), subventricular zone (SVZ), dentate gyrus (DG), CA1 and CA3 regions of hippocampus in un-operated (un-op, n = 8), sham-operated (sham-op, n = 8) and cecal ligation and puncture (CLP, n = 8) rats. # and ‡, represents differences between CLP and un-op (#, $p<0.01$) and CLP and sham-op (‡, $p<0.01$) groups, respectively.

are those that most closely simulate the clinical situation encountered in humans, recent changes in attitude towards the use of such large animals have significantly limited their use and small mammals have often been preferred as inexpensive, available and genetically similar alternatives. Peritonitis may be induced in rodents in several ways such as perforation of the bowel, inoculum of faecal material or pure bacteria cultures and CLP (Parker and Watkins 2001). The simple and reproducible CLP method has been widely used to induce peritonitis and it is more closely approximate the bacterial insult and prolonged time course of clinical infections like perforated appendicitis and diverticulitis and therefore, CLP model has been preferred to induce sepsis in the present study.

Sepsis is defined as the systemic response to a documented infection and is characterized by at least two of the following: temperature greater than 38°C or less than 36°C; heart rate greater than 90 beats per minute; respiratory rate more than 20/minute or $PaCO_2$ less than 32 mm Hg; and an alteration in white blood cell count (>12,000/mm3 or <4,000/mm3) (ACCP/SCCM 1992). Therefore, close follow-up of hemodynamic status is crucial in the diagnosis of sepsis. Although monitorization of the vital parameters consist major difficulties in rodents and hemodynamic changes may occur as systemic cytokine-induced symptoms without evidence of sepsis (Gross et al. 1993), the data obtained in the present study provided convincing evidence for the adequate simulation of sepsis in these animals. Significantly decreased arterial pressure and increased heart rate occurred concurrently with some clinical findings (e.g. piloerection, lethargy, flickering, ocular and nasal discharge) would suggest the successful induction of sepsis in the 90% of the rats used in the present study. In line with our findings, it has been previously described that the CLP procedure in rats efficiently develops cardiovascular dysfunction similar to that which occurs in human sepsis (Tang and Liu 1996, Kadoi and Goto 2004). Although we did not measure cardiac output in this study, the hemodynamic changes that we observed were consistent with those previous studies (Tang and Liu 1996, Kadoi and Goto 2004) and the changes observed in this study closely resembled the septic syndrome seen in clinical sepsis.

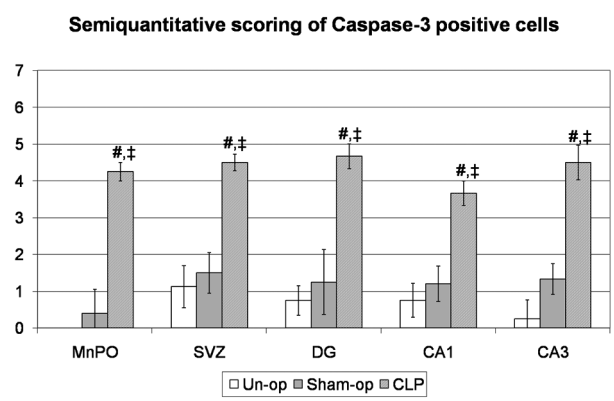

Fig. 4. A bar diagram showing the mean staining scores (±SEM) of active Caspase-3 positive cells in the median preoptic nucleus (MnPO), subventricular zone (SVZ), dentate gyrus (DG), CA1 and CA3 regions of hippocampus in un-operated (un-op, n = 8), sham-operated (sham-op, n = 8) and cecal ligation and puncture (CLP, n = 8) rats. # and ‡, represents differences between CLP and un-op (#, $p<0.01$) and CLP and sham-op (‡, $p<0.01$) groups, respectively.

SAE is a complication of sepsis and closely associated with the increased mortality of the sufferers (Sprung et al. 1990, Eidelman et al. 1996). The diagnosis of SAE based on the evaluation of the state of consciousness, changes in cognitive function and brain electrical activity recordable by EEG (Sprung et al. 1990, Young et al. 1992, Eidelman et al. 1996). More recently, SEP recordings have been used as a general test of neurologic function in septic patients (Zauner et al. 2002). Furhermore, alterations in SEP recordings in some models which the sepsis was induced by induction of pancreatitis in pigs (Ohnesorge et al. 2003) and by LPS treatment in rats (Rosengarten et al. 2007), strengthening the hypothesis that the disruption in electrical activity of brain recorded by SEP measurements could be an early indicator of progression of sepsis. Therefore, the rats in CLP group were neurologically assessed and scored, ECoG and SEP recordings were obtained for the analysis of encephalopathy and only the 50% of the rats with deteriorated neurological reflexes, increased delta frequency and prolonged SEP signals were included in CLP group in the present study. These results suggest that researchers who investigate the pathogenesis of SAE should consider assessing the indicators of cerebral dysfunction associated with inflammatory disease and be cautious to include all CLP rats within their experimental group. Although the ECoG recordings provides a large amount of data that are difficult to assess and conclude, hence it may not trigger much enthusiasm, SEP recordings that would confirm deteriorated cor-

tical signals may be useful to establish the diagnosis of SAE in animal models of sepsis.

The pathophysiology of SAE remains unclear and various mechanisms have been proposed. It's well established that apoptosis is an important mechanism during the immunopathogenesis of sepsis (Perl et al. 2007, Ayala et al. 2008) and increased apoptotic death of various parenchymal cells in various organs; e.g., endothelial cells, hepatocytes, gastrointestinal and lung epithelial cells and cardiac myocytes has been indicated in clinical and experimental sepsis (Kim et al. 2000, Mutunga et al. 2001, Coopersmith et al. 2002, Perl et al. 2005, 2007, Gambim et al. 2007, Wesche-Soldato et al. 2007, Ayala et al. 2008). However, studies that investigate its role on the brain and its associations with SAE is limited (Mouihate and Pittman 1998, Messaris et al. 2004, 2010, Sharshar et al. 2004, Semmler et al. 2005, Memos et al. 2009). Sharshar and others (2004) reported that neuronal apoptosis was more pronounced in the autonomic nuclei in septic patients and concluded that septic shock is associated with specific autonomic centers, although their patients were sedated and therefore not assessed neither for mental state and neurological deficit nor by EEG or SEP. Even though there is controversy over the relevance of endotoxin models to human sepsis, Semmler

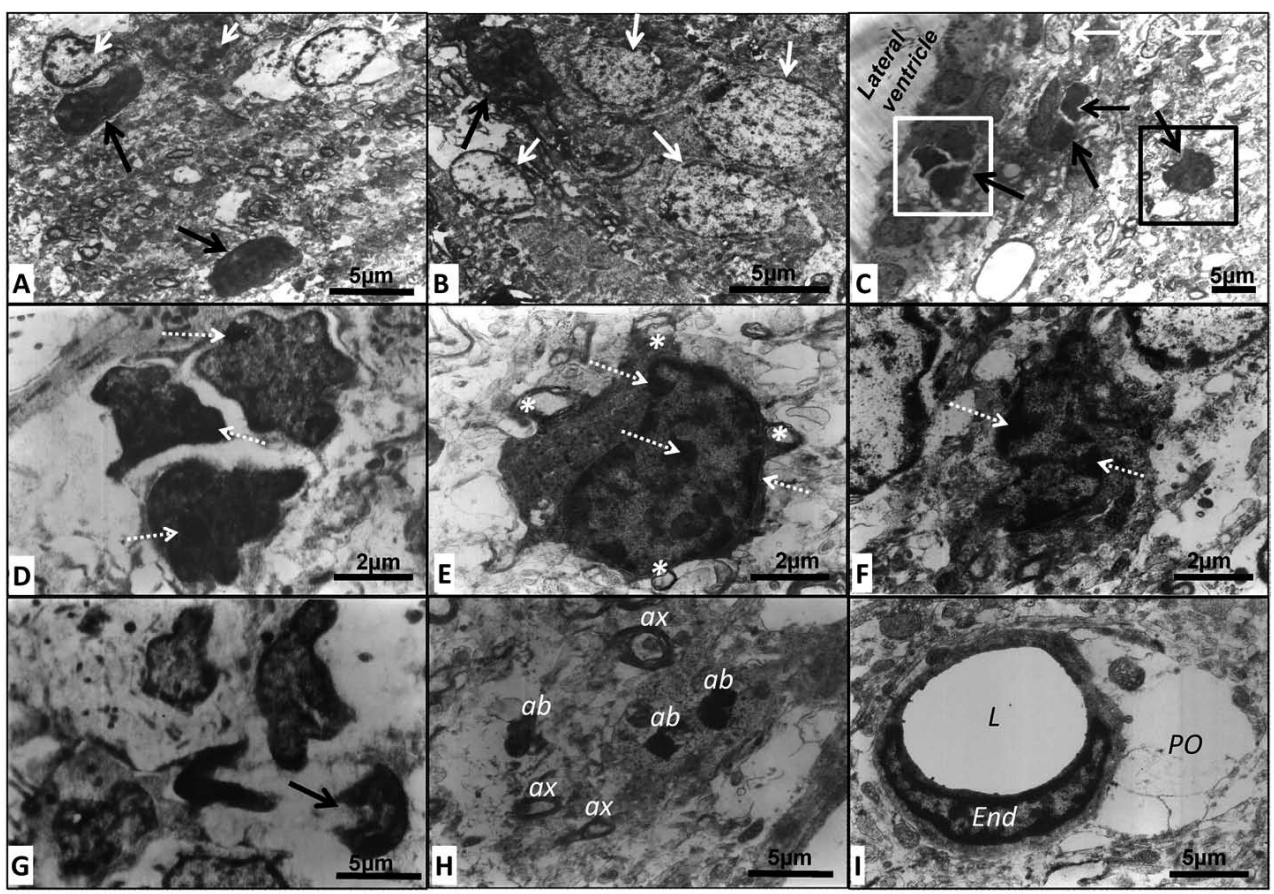

Fig. 5. Electron micrographs showing shrunken and dark atrophic cells (black arrows) interspersed between healthy looking neurons (white arrows) in CA3 **(A),** DG **(B)** and SVZ **(C)** of the CLP rats. Higher magnification of shrunken and dark cells from SVZ **(D-E)** indicated by white and black squares boxes in panel C and cells from CA1 **(F)**, usually revealed distinctive chromatin condensations (dashed white arrows), intact nuclear and cellular membrane, and cytoplasmic blebbings (asterixes), although cellular shrinkage, chromatin condensation and fragmentation was more prominent in some cells **(G)** and dying cells with disrupted cell membrane and apoptotic bodies (ab) lack a clear nuclear component and interspersed around myelinated axons (ax) was also observed **(H)**. An electron micrograph showing an endothelial cell (End) and lumen (L) of a capillary with discernable perimicrovascular edema (PO) **(I)**.

and coworkers (2005) proposed a sepsis-induced time-dependent increase in the number of apoptotic cells in the brains of rats that received lipopolysaccharide and suggested hippocampus as the most vulnerable brain region, although significantly increased number of cells were also reported in cerebral cortex, cerebellum and the midbrain (Sharshar et al., 2004). Unlike Semmler and coauthors (2005), Mouihate and Pittman (1998) found no evidence of apoptosis in the hippocampus, hypothalamus, area postrema, subfornical organ, organum vasculosum of the lamina terminalis and nucleus tractus solitaris of the rats treated with acute (5.5 hour) or chronic (5 days) intraperitoneal (i.p.) administration and central injection of LPS. The reasons for these pronounced differences are not clear but may be due to the variety of factors such as the differences in the ages or phenotype of the animals investigated, tissue preparation techniques, methods of quantification. Increased apoptosis in neurons of the CA1 region of the hippocampus, choroid plexus and Purkinje cells of the cerebellum have also been reported in another widely used rat model of sepsis; CLP model (Messaris et al. 2004), which we have also been preferred in our study. However, vital findings or the brains' electrical activity were not monitored and thus development of sepsis and SAE were not confirmed in these studies, while only the rats that developed the signs and symptoms of sepsis and SAE were included in CLP group in our study. These results suggests that the future studies that compare the progression of apoptosis in the CLP rats with confirmed SAE findings to those do not, would provide crucial information about the sequence of events in sepsis and SAE, and the correlation of apoptosis with those syndromes.

Significantly increased apoptosis in hippocampal regions in the present study would suggest that this particular region may be more vulnerable to inflammatory and/or circulatory changes observed in the brain. It has been previously reported that rats survived and fully recovered 10 days after CLP demonstrated impaired spatial learning and memory (Barichello et al. 2005) and some cognitive skills, such as memory, did not completely improve in most of the sepsis patient at one-year follow up (Heyland et al. 2000). Thus, it's tempting to suggest that the increased apoptotic cell death in CA1, CA3 and DG of these rats may underlie at least some of this impairment, since it's well-established that the hippocampal formation plays important role in spatial learning and memory in rats (Morris et al. 1982). DG of the hippocampus and the SVZ of the lateral ventricles, in which significantly increased apoptosis was observed in the present study, have also been established as the primary sites of adult neurogenesis (Zhao et al. 2008) and inflammation was proposed as a new candidate in modulating adult neurogenesis although its effects are in debate (Das and Basu 2008). Since most of the CNS insults lead to increased proliferation of progenitors in these neurogenic areas (Zhao et al. 2008), another possible explanation of the increased apoptosis in DG and SVZ observed in the present study may be the outcome of an increased neurogenesis and elimination of supernumerous cells from neurogenic regions by apoptosis to contribute to a self-renewal mechanism in the brain. Research is currently underway with an objective to seek answers to the question whether neurogenesis is in fact triggered and counterbalanced by an accompanying cell death in the same regions in CLP rats.

Significantly increased number of apoptotic cells found in MnPO of CLP rats is another novel finding of the present study. MnPO constitutes the most anterior part of the anterior wall of the third ventricle, together with two circumventricular organs (CVOs); the subfornical organ and the organum vasculosum of the lamina terminalis. CVOs of the lamina terminalis lacks blood-brain barrier and has been shown to be influenced by hormonal, ionic and peptide composition of the blood and are clearly established as the most important cerebral targets for both circulating peptides such as angiotensin II, atrial natriuretic peptide and relaxin (McKinley et al. 1999) and antihypertensive chemicals such as angiotensin II receptor blockers (Ployngam et al. 2009). The information received by CVOs is then integrated in MnPO and neural output from the MnPO is relayed to a number of effector regions including supraoptic and paraventricular nucleus involved in maintaining body fluid and cardiovascular homeostasis (McKinley et al. 2004, Stocker and Toney 2005). In addition, a pivotal role has also been implied for MnPO in the integration of thermal and osmotic information (Honda et al. 1990, Whyte and Johnson 2005). Thus, our findings may suggest that hemodynamic failure observed in CLP rats in the present study may be fostered by neuronal apoptosis in the MnPO, which has been regarded as the "headquater for control of body fluid hemostasis" (McKinley et al. 2004) together with the CVOs that are known to be vulnerable to systemic

challenge. Or alternatively, systemic challenge develops in sepsis may exert its deteriorating effects on MnPO through CVOs, which in turn would then the progression of the septic challenge and irreversible phase of the disease develops.

CONCLUSION

In conclusion, the present investigation revealed significantly higher number of apoptotic cells in the brain regions with crucial regulatory functions in rats with confirmed sepsis and SAE. Although it would be premature to attempt to draw any strict parallels between the brain dysfunction observed in human beings suffering from sepsis and the structural abnormalities observed in CLP rat model of sepsis, the material provided here renders a valuable reference point for future analyses of possible apoptotic cell death observed in patients with sepsis. These results would further suggest that therapeutic efforts aimed at blocking apoptosis may represent an important target for critically ill patients with sepsis and SAE.

ACKNOWLEDGMENTS

The work was supported by Uludag University (Grant no: T-2006/24).

REFERENCES

Aird WC (2003) The role of the endothelium in severe sepsis and multiple organ dysfunction syndrome. Blood 101: 3765–3777.

ACCP/SSCM [American College of Chest Physicians/ Society of Critical Care Medicine Consensus Conference] (1992) Definitions for sepsis and organ failure and guidelines for the use of innovative therapies in sepsis. Crit Care Med 20: 864–874.

Ari I, Kafa IM, Kurt MA (2006) Perimicrovascular edema in the frontal cortex in a rat model of intraperitoneal sepsis. Exp Neurol 198: 242–249.

Ayala A, Perl M, Venet F, Lomas-Neira J, Swan R, Chung CS (2008) Apoptosis in sepsis: mechanisms, clinical impact and potential therapeutic targets. Curr Pharm Des 14: 1853–1859.

Barichello T, Martins MR, Reinke A, Feier G, Ritter C, Quevedo J, Dal-Pizzol F (2005) Cognitive impairment in sepsis survivors from cecal ligation and perforation. Crit Care Med 33: 221–223.

Basler T, Meier-Hellmann A, Bredle D, Reinhart K (2002) Amino acid imbalance early in septic encephalopathy. Intensive Care Med 28: 293–298.

Booke M, Westphal M, Hinder F, Traber LD, Traber DL (2003) Cerebral blood flow is not altered in sheep with Pseudomonas aeruginosa sepsis treated with norepinephrine or nitric oxide synthase inhibition. Anesth Analg 96: 1122–1128.

Bowton DL, Bertels NH, Prough DS, Stump DA (1989) Cerebral blood flow is reduced in patients with sepsis syndrome. Crit Care Med 17: 399–403.

Consales G, De Gaudio AR (2005) Sepsis associated encephalopathy. Minerva Anestesiol 71: 39–52.

Coopersmith CM, Stromberg PE, Dunne WM, Davis CG, Amiot DM 2nd, Buchman TG, Karl IE, Hotchkiss RS (2002) Inhibition of intestinal epithelial apoptosis and survival in a murine model of pneumonia-induced sepsis. JAMA 287: 1716–1721.

Das S, Basu A (2008) Inflammation: A new canditate in modulating adult neurogenesis. J Neurosci Res 86: 1199–1208.

Davies DC, Parmar NK, Moss R, Tighe D, Bennett ED (2001) The role of the adrenergic system in septic encephalopathy. Crit Care 5: 180–185.

Davies DC (2002) Blood brain barrier breakdown in septic encephalopathy and brain tumours. J Anat 200: 639–646.

Doods WJ (1982) The pig model for biomedical research. Fed Proc. 41: 292–297

Eidelman LA, Putterman D, Putterman C, Sprung CL (1996) The spectrum of septic encephalopathy. Definitions, etiologies, and mortalities. J Am Med Assoc 275: 470–473.

Fink MP, Heard SO (1990) Laboratory models of sepsis and septic shock. J Surg Res 49: 186–196.

Freund HR, Muggia-Sullam M, Peiser J, Melamed E (1985) Brain neurotransmitter profile is deranged during sepsis and septic encephalopathy in the rat. J Surg Res 38: 267–271.

Gambim MH, Carmo AO, Marti L, Verissimo-Filho S, Lopes LR, Janiszewski M (2007) Platelet-derived exosomes induce endothelial cell apoptosis through peroxynitrite generation: experimental evidence for a novel mechanism of septic vascular dysfunction. Crit Care 11: R107.

Garrido AG, Poli de Figueiredo LF, Rocha Silva M (2004) Experimental models of sepsis and septic shock: an overview. Acta Cir Bras 19: 82–88.

Gross V, Leser HG, Heinish H, Schölmerich J (1993) Inflammatory mediators and cytokines: new aspects of

the pathophysiology and assessment of severity of acute pancreatitis? Hepatogastroenterelogy 40: 522–530.

Habernam ZL, von den Brom WE, Venker-van Haagen AJ, Baumans V, de Groot HNM, Hellebrekers LJ (1999) EEG evaluation of reflex testing as assessment of depth of pentobarbital anaesthesia in the rat. Lab Anim 33: 47–57.

Heyland DK, Hopman W, Coo H, Tranmer J, McColl MA (2000) Long-term health-related quality of life in survivors of sepsis. Short Form 36: a valid and reliable measure of health-related quality of life. Crit Care Med 28: 3599–3605.

Honda H, Negoro H, Dyball REJ, Higuchi T, Takano S (1990) The osmoreceptor complex in the rat: evidence for interactions between the supraoptic and other diencephalic nuclei. J Physiol 431: 225–241.

Hotchkiss RS, Long RC, Hall JR, Shires GT, Brouillard, RG, Millikan WJ, Jones DP (1989) An in vivo examination of rat brain during sepsis with 31P-NMR spectroscopy. Am J Physiol 257: C1055–C1061.

Kadoi Y, Saito S, Kunimoto F, Imai T, Fujita T (1996) Impairment of the brain beta-adrenergic system during experimental endotoxemia. J Surg Res 61: 496–502.

Kadoi Y, Goto F (2004) Selective inducible nitric oxide inhibition can restore hemodynamics, but does not improve neurological dysfunction in experimentally-induced septic shock in rats. Anesth Analg 99:212–20.

Kafa IM, Ari I, Kurt MA (2007) The peri-microvascular edema in hippocampal CA1 area in a rat model of sepsis. Neuropathology 27: 213–220.

Kim YM, Kim TH, Chung HT, Talanian RV, Yin XM, Billiar TR (2000) Nitric oxide prevents tumor necrosis factor alpha-induced rat hepatocyte apoptosis by the interruption of mitochondrial apoptotic signaling through S-nitrosylation of caspase-8. Hepatology 32: 770–778.

Kinasewitz GT, Chang ACK, Peer GT, Hinshaw LB, Taylor FB (2000) Peritonitis in the baboon: a primate model which simulates human sepsis. Shock 13: 100–109.

Lam C, Tyml K, Martin C, Sibbald W (1994) Microvascular perfusion is impaired in a rat model of normotensive sepsis. J Clin Invest 94: 2077–2083.

McCuskey RS, Urbaschek R, Urbaschek B (1996) The microcirculation during endotoxemia. Cardiovasc Res 32: 752–763.

McGilvray ID, Rotstein OD (1998) Role of the coagulation system in the local and systemic inflammatory response. World J Surg 22: 179–186.

McKinley MJ, Gerstberger R, Mathai ML, Oldfield BJ, Schmid H (1999) The lamina terminalis and its role in fluid and electrolyte homeostasis. J Clin Neurosci 6: 289–301.

McKinley MJ, Mathai, ML, McAllen RM, McClear RC, Miselis RR, Pennington GL, Vivas L, Wade JD, Oldfield BJ (2004) Vasopressin secretion: osmotic and hormonal regulation by the lamina terminalis. J Neuroendocrinol 16: 340–347.

Memos N, Betrosian A, Messaris E, Boutsikou M, Kataki A, Chatzigianni E, Nikolopoulou M, Leandros E, Konstadoulakis M (2009) Administration of human protein-C concentrate prevents apoptotic brain cell death after experimental sepsis. Brain Res 1264: 119–126.

Messaris E, Memos N, Chatzigianni E, Konstadoulakis MM, Menenakos E, Katsaragakis S, Voumvourakis C, Androulakis G (2004) Time-dependent mitochondrial mediated programmed neuronal cell death prolongs survival in sepsis. Crit Care Med 32: 1764-1770.

Messaris E, Betrosian A, Memos N, Chatzigianni E, Boutsikou M, Economou V, Dontas I, Theodossiades G, Konstadoulakis MM, Douzinas EE (2010) Administration of human protein C improves survival in an experimental model of sepsis. Crit Care Med 38: 209–216.

Morris RG, Garrud P, Rawlins JN, O'Keefe J (1982) Place navigation impaired in rats with hippocampal lesions. Nature 297: 681–683.

Mouihate A, Pittman QJ (1998) Lipopolysaccharide-induced fever is dissociated from apoptotic cell death in the rat brain. Brain Res 805: 95–103.

Mutunga M, Fulton B, Bullock R, Batchelor A, Gascoigne A, Gillespie JI, Baudouin SV (2001) Circulating endothelial cells in patients with septic shock. Am J Respir Crit Care Med 163: 195–200.

Natanson C, Esposito CJ, Banks SM (1998) The sirens' song of confirmatory sepsis trials: selection bias and sampling error. Crit Care Med 26: 1927–1931.

Ohnesorge H, Bischoff P, Scholz J, Yekebas E, Shulte am Esch J (2003) Somatosensory evoked potentials as predictor of systemic inflammatory response syndrome in pigs? Intensive Care Med 29: 801–807.

Orlikowski D, Chazaud B, Plonquet A, Poron F, Sharshar T, Maison P, Raphaël JC, Gherardi RK, Créange A (2003) Monocyte chemoattractant protein 1 and chemokine receptor CCR2 productions in Guillain-Barre syndrome and experimental autoimmune neuritis. J Neuroimmunol 134: 118–127.

Papadopoulos MC, Davies DC, Moss RF, Tighe D, Bennett ED (2000) Pathophysiology of septic encephalopathy: a review. Crit Care Med 28: 3019–3024.

Parker SJ, Watkins PE (2001) Experimental models of gram-negative sepsis. Br J Surg 88: 22–30.

Paxinos G, Watson C (1997) The rat brain in stereotaxic coordinates (3rd edition). Academic Press, New York, USA.

Perl M, Chung CS, Lomas-Neira J, Rachel TM, Biffl WL, Cioffi WG, Ayala A (2005) Silencing of fas, but not caspase-8, in lung epithelial cells ameliorates pulmonary apoptosis, inflammation, and neutrophil influx after hemorrhagic shock and sepsis. Am J Pathol 167: 1545–1559.

Perl M, Chung CS, Swan R, Ayala A (2007) Role of programmed cell death in the Immunopathogenesis of sepsis. Drug Discov Today Dis Mech 4: 223–230.

Ployngam T, Katz SS, Collister JP (2010) Role of the median preoptic nucleus in chronic hypotensive effect of losartan in sodium-replete normal rats. Clin Exp Pharmacol Physiol 37: 7–13.

Rahman A, Anwar KN, True AL, Malik AB (1999) Thrombin-induced p65 homodimer binding to downstream NK-kappa B site of the promoter mediates endothelial ICAM-1 expression and neutrophil adhesion. J Immunol 162: 5466–5476.

Rosengarten B, Hecht M, Auch D, Ghofrani HA, Schermuly RT, Grimminger F, Kaps M (2007) Microcirculatory dysfunction in the brain preceded changes in evoked potentials in endotoxin-induced sepsis syndrome in rats. Cerebrovasc Dis 23: 140–147.

Semmler A, Okulla T, Sastre M, Dumitrescu-Ozimek L, Heneka MT (2005) Systemic inflammation induces apoptosis with variable vulnerability of different brain regions. J Chem Neu 30: 144–157.

Sharshar T, Annane D, de laGrandmaison GF, Brouland JP, Hopkinson NS, Gray F (2004) The neuropathology of septic shock. Brain Pathol 14: 21–33

Siami S, Annane D, Sharshar T (2008) The encephalopathy in sepsis. Crit Care Clin 24: 67–82.

Soejima Y, Fujii Y, Ishikawa T, Takeshita H, Maekawa T (1990) Local cerebral glucose utilization in septic rats. Crit Care Med 18: 423–427.

Sprung CL, Peduzzi PN, Shatney CH, Schein RM, Wilson MF, Sheagren JN, Hinshaw LB (1990) Impact of encephalopathy on mortality in the sepsis syndrome. Crit Care Med 18: 801–806.

Stocker SD, Toney GM (2005) Median preoptic neurones projecting to the hypothalamic paraventricular nucleus respond to osmotic, circulating Ang II and baroreceptor input in the rat. J Physiol 568: 599–615.

Sugama Y, Tiruppathi C, Offakidevi K, Andersen TT, Fenton JW, Malik AB (1992) Thrombin-induced expression of endothelial P-selectin and intercellular adhesion molecule-1: a mechanism for stabilizing neutrophil adhesion. J Cell Biol 119: 935–944.

Tang C, Liu MS (1996) Initial externalization followed by internalization of beta-adrenergic receptors in rat heart during sepsis. Am J Physiol 270: R254–R263.

Terborg C, Schummer W, Albrecht M, Reinhart K, Weiller C, Rother J (2001) Dysfunction of vasomotor reactivity in severe sepsis and septic shock. Intensive Care Med 27: 1231–1234.

Wesche-Soldato DE, Chung CS, Gregory SH, Salazar-Mather TP, Ayala CA, Ayala A (2007) CD8+ T cells promote inflammation and apoptosis in the liver after sepsis: role of Fas-FasL. Am J Pathol 171: 87–96.

Whyte DG, Johnson AK (2005) Thermoregulatory role of periventricular tissue surrounding the anteroventral third ventricle (AV3V) during acute heat stress in the rat. Clin Exp Pharmacol Phsiol 32: 457–461.

Wichterman KA, Baue AE, Chaudry IH (1980) Sepsis and septic shock-a review of laboratory models and a proposal. J Surg Res 29: 189–201.

Wijdicks EF, Stevens M (1992) The role of hypotension in septic encephalopathy following surgical procedures, Arch Neurol 49: 653–656.

Wilson JX, Young GB (2003) Progress in clinical neurosciences: sepsis-associated encephalopathy: evolving concepts. Can J Neurol Sci 30: 98–105.

Winder TR, Minuk GY, Sargeant EJ, Seland TP (1988) Gamma-aminobutyric acid (GABA) and sepsis-related encephalopathy. Can J Neurol Sci 15: 23–25.

Xu G, Zhang W, Bertram P, Zheng XF, McLeod H (2004) Pharmacogenomic profiling of the PI3K/PTEN-AKT-mTOR pathway in common human tumors. Int J Oncol 24: 893–900.

Young GB, Bolton CF, Archibald YM, Austin TW, Wells GA (1992) The encephalogram in sepsis-associated encephalopathy. J Clin Neurophysiol 9: 145–152.

Zauner C, Gendo A, Kramer L, Funk GC, Bauer E, Schenk P, Ratheiser K, Madl C (2002) Impaired subcortical and cortical sensory evoked potential pathways in septic patients. Crit Care Med 30: 1136–1139.

Zhao C, Deng W, Gage FH (2008) Mechanisms and functional implications of adult neurogenesis. Cell 132: 645–660.